arXiv:1503.02125v3 [hep-ph] 5 Sep 2015

# Photoproduction of the charged charmoniumlike $Z_c^+(4200)$

Xiao-Yun Wang[1,2,3*] and Xu-Rong Chen[1,3]
[1] *Institute of Modern Physics, Chinese Academy of Sciences, Lanzhou 730000, China*
[2] *University of Chinese Academy of Sciences, Beijing 100049, China*
[3] *Research Center for Hadron and CSR Physics, Institute of Modern Physics of CAS and Lanzhou University, Lanzhou 730000, China*

Alexey Guskov[†]
[1] *Joint Institute for Nuclear Research, Dubna 141980, Russia*

In this work, inspired by the observation of charmoniumlike $Z_c^+(4200)$, we study the photoproduction of charged charmoniumlike $Z_c^+(4200)$ with an effective Lagrangian approach and the Regge trajectories model. The numerical results indicate that the Reggeized treatment can lead to a lower total cross section of the $Z_c^+(4200)$ photoproduction and the peak position of cross section was moved to the higher energy point when the Reggeized treatment was added. Moreover, using the data from the COMPASS experiment and presented theoretical predictions, an upper limit of the decay width of $Z_c(4200) \to J/\psi\pi$ is estimated. The relevant results not only shed light on the further experiment of searching for the charmoniumlike $Z_c(4200)$ state via meson photoproduction, but also provide valuable informations for having a better comprehension of the nature of charmoniumlike $Z_c(4200)$ state.

PACS numbers: 13.60.Le, 11.10.Ef, 11.55.Jy, 12.40.Vv

## I. INTRODUCTION

As of now, most of hadrons can be well described by the classical constituent quark model in the picture of $q\bar{q}$ for mesons and $qqq$ for baryons. However, according to the quantum chromodynamics, the exotic states (such as the multiquark states, molecule states etc.) are also allowed to exist in our Universe. Therefore, searching and explaining these exotic states arouse great interest among researchers.

In the experiments, a series of charmoniumlike and bottomoniumlike states referred to $XYZ$ have been observed [1–16]. Especially, those charged $Z$ states are even more exotic since they have a minimal quark content of $\left|c\bar{c}u\bar{d}\right\rangle$ ($Z_c^+$) or $\left|b\bar{b}u\bar{d}\right\rangle$ ($Z_b^+$) [17–21]. Later, some neutral $Z$ states (including $Z_c^0(3900)$, $Z_b^0(10610)$ and $Z_c^0(4020)$) were reported by experiments [22–24], which provide important informations of confirming and understanding the exotic $Z$ states.

On theoretical aspects, these exotic states are interpreted as a hadronic molecule, a tetraquark, hadrocharmonium or just a cusp effect. [17–21, 25–43], *et al.* Moreover, several hidden charm baryons composed by $|c\bar{c}qqq\rangle$ have been predicted and investigated [44–47]. These studies enriched the picture of exotic states.

Recently, Belle Collaboration claimed that a new charged charmoniumlike $Z_c^+(4200)$ was observed in the invariant mass spectrum of $J/\psi\pi^+$ with a significance of $6.2\sigma$ [13]. Its mass and width are $M_{Z_c(4200)} = 4196^{+31+17}_{-29-13}$ MeV/$c^2$ and $\Gamma_{Z_c(4200)} = 370^{+70+70}_{-70-132}$ MeV [13], respectively. Meanwhile, the quantum number of $Z_c^+(4200)$ was determined to be $J^P = 1^+$ since other hypotheses with $J^P \in \{0^-, 1^-, 2^-, 2^+\}$ were excluded [13]. In Ref. [40], the calculations show that $Z_c(4200)$ is a strong candidate of the lowest axial-vector tetraquark state within the framework of the color-magnetic interaction. In Refs. [41–43], using the QCD sum rule approach, the relevant results also support the tetraquark interpretation of $Z_c(4200)$. Besides, the $Z_c(4200)$ was described as a molecule-like state in [48]. The above informations indicate that the $Z_c(4200)$ is an ideal candidate for investigating the nature of exotic charmoniumlike states.

As of now, the charmoniumlike $XYZ$ states are only observed in four ways [17], i.e., the $e^+e^-$ annihilation ($e^+e^- \to XYZ$ or $e^+e^- \to J/\psi + XYZ$), $\gamma\gamma$ fusion process ($\gamma\gamma \to XYZ$), $B$ meson decay ($B \to K + XYZ$) and hidden-charm dipion decays of higher charmonia or charmoniumlike states. Therefore, searching for the charmoniumlike states through other production process is an important topic, which will be useful in confirming and understanding these exotic $XYZ$ states. For example, Ke *et al.* suggested to search for the charged $Z_c^\pm(4430)$ by the nucleon-antinucleon scattering [49], while the production of neutral $Z_c^0(4430)$ and $Z_c^0(4200)$ states in $\bar{p}p$ reaction were investigated in Refs. [50, 51]. Moreover, in Refs. [52–55], the meson photoproduction process were proposed to be an effective way to search for the charmoniumlike states. Soon after, according to the theoretical predictions obtained in Ref. [54], an experiment of searching for the $Z_c^\pm(3900)$ through $\gamma N \to Z_c^\pm(3900)N \to J/\psi\pi^\pm N$ was carried out by the COMPASS Collaboration [56]. Unfortunately, no signal of exclusive photoproduction of the $Z_c^\pm(3900)$ state and its decay into $J/\psi\pi^\pm$ was found. Thus it is important to discuss whether there are other charmoniumlikes that have a discovery potential through $\gamma N \to J/\psi\pi^\pm N$ channel. Besides, a more accuracy theoretical prediction is necessary.

Usually, for the meson photoproduction process, the mesonic Reggeized treatment will play important role at high photo energies. The exchange of dominant meson Regge trajectories already used to successfully describe the meson photoproduction in Refs. [57–59]. Since a high photon beam energy is required for the production of charmoniumlike states

---

[*] xywang@impcas.ac.cn
[†] avg@jinr.ru

through meson photoproduction process, the Reggeized treatment will be necessary to ensure the result accuracy. In this work, within the frame of an effective Lagrangian approach and the Regge trajectories model, we systematically study the production of charged $Z_c(4200)$ by meson photoproduction process in order to provide a reliable theoretical results and shed light on our understanding of the properties and production mechanism of charged $Z_c(4200)$ state.

This paper is organized as follows. After an introduction, we present the investigate method and formalism. The numerical result and discussion are given in Sec. III. In Sec. IV, we discuss the upper limit of decay width of $Z_c(4200) \to J/\psi\pi$. Finally, this paper ends with a brief conclusion.

## II. FORMALISM AND INGREDIENTS

Since the $Z_c(4200)$ have a strong coupling with $J/\psi\pi$ [13, 40, 43], the photoproduction process $\gamma p \to Z_c^+(4200)n \to J/\psi\pi^+n$ may be an ideal reaction channel of searching and studying production of the charged $Z_c^+(4200)$. Moreover, considering the signal of $Z_c^+(4200)$ are mainly from the contributions of $\pi$ exchange, while the contributions from $\rho$ and $a_0$ exchange can be negligible[1], the process as depicted in Fig. 1 are regard as the source of signal of $Z_c^+(4200)$. Besides, the reaction $\gamma p \to J/\psi\pi^+n$ via Pomeron exchange (as shown in Fig.2) are also calculated, which is considered to be the background for the $Z_c^+(4200)$ photoproduction. To investigate $Z_c^+(4200)$ production, an effective Lagrangian approach and the Regge trajectories model in terms of hadrons will be used in the follows.

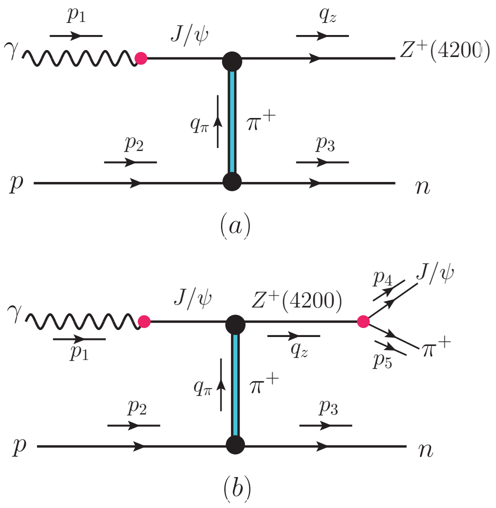

FIG. 1: (Color online) The Feynman diagram for $\gamma p \to Z_c^+(4200)n$ reaction (a) and $\gamma p \to J/\psi\pi^+n$ reaction (b) through $\pi$ exchange.

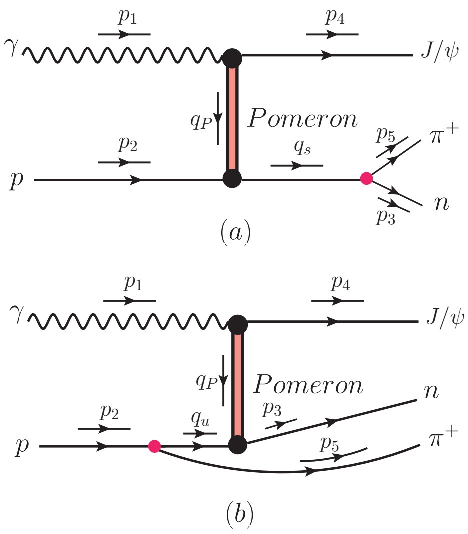

FIG. 2: (Color online) The Feynman diagram of $\gamma p \to J/\psi\pi^+n$ process through the Pomeron exchange.

### A. Feynman diagrams and effective interaction Lagrangian densities

Fig. 1 show the basic tree level Feynman diagram for the production of $Z_c^+(4200)$ in $\gamma p \to Z_c^+(4200)n \to J/\psi\pi^+n$ reaction via pion exchange. To gauge the contributions of these diagrams, we need to know the effective Lagrangian densities for each interaction vertex.

For the interaction vertex of $\pi NN$, we use the effective pseudoscalar coupling [2] [68–70],

$$\mathcal{L}_{\pi NN} = -ig_{\pi NN}\bar{N}\gamma_5\vec{\tau}\cdot\vec{\pi}N \tag{1}$$

where $N$ and $\pi$ stand for the fields of nucleon and pion meson, while $\vec{\tau}$ is the Pauli matrix. The coupling constant of the $\pi NN$ interaction was given in many theoretical works, and we take $g^2_{\pi NN}/4\pi = 14.4$ [71].

As mentioned above, the spin-parity of $Z_c^+(4200)$ has been determined by Belle Collaboration to be $J^P = 1^+$ [13]. Thus the relevant effective Lagrangian for the vertex[3] of $Z\psi\pi$ read as [52],

---

[1] In Refs. [60–62], the results indicate that the pion exchange plays a major role in the $\gamma p \to Xn$ process by analyzing the HERA data. Besides, In Refs. [63, 64], it is found that the contributions of $\rho$ and $a_0$ exchange in the $\gamma^* p \to Xn$ reaction are very small. Thus, in the present work we only consider the contribution from the one pion exchange. Here, the $\gamma^*$ stand for the virtual photon.

[2] It should be noted that some works [65, 66] have pointed out that the simple pseudoscalar coupling between nucleons and pions is incomplete and inconsistent with chiral symmetry. Thus the pseudovector coupling is suggested in Refs. [65, 66]. However, since the new pseudovector formalism may not yet be ready for phenomenological use [67], the pseudoscalar coupling is adopted in the present work.

[3] For the sake of simplicity, we use $Z$ and $\psi$ denote $Z_c(4200)$ and $J/\psi$, respectively.

$$\mathcal{L}_{Z\psi\pi} = \frac{g_{Z\psi\pi}}{M_Z}(\partial^\mu\psi^\nu\partial_\mu\pi Z_\nu - \partial^\mu\psi^\nu\partial_\nu\pi Z_\mu), \tag{2}$$

where $Z$, and $\psi$ denote the fields of $Z(4200)$ and $J/\psi$ meson, respectively. With the effective Lagrangians above, the coupling constant $g_{Z\psi\pi}$ can be determined by the partial decay widths $\Gamma_{Z_c(4200)\to J/\psi\pi}$,

$$\begin{aligned}\Gamma_{Z(4200)\to J/\psi\pi} &= \left(\frac{g_{Z\psi\pi}}{M_Z}\right)^2 \frac{|\vec{p}_\pi^{\,\mathrm{c.m.}}|}{24\pi M_Z^2} \\ &\quad\times\left[\frac{(M_Z^2-m_\psi^2-m_\pi^2)^2}{2}+m_\psi^2E_\pi^2\right],\end{aligned} \tag{3}$$

with

$$|\vec{p}_\pi^{\,\mathrm{c.m.}}| = \frac{\lambda^{1/2}(M_Z^2,m_\psi^2,m_\pi^2)}{2M_Z}, \tag{4}$$

$$E_\pi = \sqrt{|\vec{p}_\pi^{\,\mathrm{c.m.}}|^2+m_\pi^2}, \tag{5}$$

where $\lambda$ is the Källen function with $\lambda(x,y,z)=(x-y-z)^2-4yz$.

As of now, no relevant experiment datas about $\Gamma_{Z(4200)\to J/\psi\pi}$ can be available [72]. However, in Ref. [43], the authors obtained the partial decay width $\Gamma_{Z_c(4200)\to J/\psi\pi} = 87.3\pm 47.1$ MeV with the QCD sum rule approach, which allow us to estimate the lower (upper) limit of the decay width of $Z(4200)\to J/\psi\pi$, $\Gamma_{Z(4200)\to J/\psi\pi} = 40.2(134.4)$ MeV. With $M_Z = 4196$ MeV/$c^2$ and $\Gamma_Z = 370$ MeV [72], we get $g_{Z\psi\pi}/M_z = 1.174, 1.731, 2.147$ MeV, which correspond to three typical partial decay width $\Gamma_{Z(4200)\to J/\psi\pi} = 40.2, 87.3, 134.4$ MeV, respectively.

For the interaction vertex of $Z\gamma\pi$, we need to derive it by the vector meson dominance (VMD) mechanism [73–75]. In the VMD mechanism for photoproduction, a real photon can fluctuate into a virtual vector meson, which subsequently scatters off the target proton. Thus within the frame of VMD mechanism, we get the Lagrangian of depicting the coupling of the intermediate vector meson $J/\psi$ with a photon as follows,

$$\mathcal{L}_{J/\psi\gamma} = -\frac{em_\psi^2}{f_\psi}V_\mu A^\mu, \tag{6}$$

where $m_\psi^2$ and $f_\psi$ are the mass and the decay constant of $J/\psi$ meson, respectively. With the above equation, one gets the expression for the $J/\psi\to e^+e^-$ decay,

$$\Gamma_{J/\psi\to e^+e^-} = \left(\frac{e}{f_\psi}\right)^2\frac{8\alpha\left|\vec{p}_e^{\,\mathrm{c.m.}}\right|^3}{3m_\psi^2}, \tag{7}$$

where $\vec{p}_e^{\,\mathrm{c.m.}}$ indicate the three-momentum of an electron in the rest frame of the $J/\psi$ meson, while $\alpha = e^2/4\hbar c = 1/137$ is the electromagnetic fine structure constant. Thus, in the light of the partial decay width of $J/\psi\to e^+e^-$ [72]

$$\Gamma_{J/\psi\to e^+e^-} \simeq 5.547\ \mathrm{keV}, \tag{8}$$

we get the constant $e/f_\psi \simeq 0.027$.

In Fig. 2, we present the Feynman diagram for the $\gamma p\to J/\psi\pi^+n$ process through Pomeron exchange, which is considered as the main background contributions to $\gamma p\to Z_c^+(4200)n\to J/\psi\pi^+n$ process. To depict the Pomeron exchange process, the relevant formulas which were used in Refs. [52, 76, 77] are adopted in this work. The Pomeron-nucleon coupling is described as follow,

$$F_\mu(t) = \frac{3\beta_0(4m_N^2-2.8t)}{(4m_N^2-t)(1-t/0.7)^2}\gamma_\mu = F(t)\gamma_\mu, \tag{9}$$

where $t = q_{\mathcal{P}}^2$ is the exchanged Pomeron momentum squared. $\beta_0^2 = 4$ GeV$^2$ stands for the coupling constant between a single Pomeron and a light constituent quark.

For the vertex of $\gamma\psi\mathcal{P}$, with an on-shell approximation for keeping the gauge invariance, we have

$$V_{\gamma\psi\mathcal{P}} = \frac{2\beta_c\times 4\mu_0^2}{(m_\psi^2-t)(2\mu_0^2+m_\psi^2-t)}T_{\mu\rho\nu}\epsilon_\psi^\nu\epsilon_\gamma^\mu\mathcal{P}^\rho, \tag{10}$$

with

$$\begin{aligned}T^{\mu\rho\nu} &= (p_1+p_4)^\rho g^{\mu\nu} - 2p_1^\nu g^{\rho\mu} \\ &\quad+2\Big\{p_1^\mu g^{\rho\nu} + \frac{p_4^\nu}{p_4^2}(p_1\cdot p_4 g^{\rho\mu} - p_1^\rho p_4^\mu - p_1^\mu p_4^\rho) \\ &\quad-\frac{p_1^2p_4^\mu}{p_4^2 p_1\cdot p_4}(p_4^2g^{\rho\nu} - p_4^\rho p_4^\nu)\Big\} + (p_1-p_4)^\rho g^{\mu\nu},\end{aligned} \tag{11}$$

where $\beta_c^2 = 0.8$ GeV$^2$ is the effective coupling constant between a Pomeron and a charm quark within $J/\psi$ meson, while $\mu_0 = 1.2$ GeV$^2$ denotes a cutoff parameter in the form factor of Pomeron.

### B. Cross sections for the $\gamma p\to Z_c^+(4200)n$ reaction

After the above preparations, the invariant scattering amplitude $\mathcal{A}$ for the $\gamma(p_1)p(p_2)\to Z_c^+(4200)(q_z)n(p_3)$ reaction by exchanging a $\pi$ meson read as,

$$\begin{aligned}\mathcal{A} &= (\sqrt{2}g_{\pi NN}\frac{g_{Z\psi\pi}}{M_Z}\frac{e}{f_\psi})\bar{u}(p_3)\gamma_5u(p_2)\epsilon_Z^{*\mu} \\ &\quad\times\epsilon_\gamma^\nu\left[p_1\cdot(q_z-p_1)g_{\mu\nu} - p_{1\mu}(q_z-p_1)_\nu\right] \\ &\quad\times\frac{1}{q_\pi^2-m_\pi^2}F_{\pi NN}(q_\pi^2)F_{Z\psi\pi}(q_\pi^2)\end{aligned} \tag{12}$$

where $F_{\pi NN}(q_\pi^2)$ and $F_{Z\psi\pi}(q_\pi^2)$ are the form factors for the vertices of $\pi NN$ and $Z\psi\pi$, respectively. We have the following definitions for both form factors,

$$F_{\pi NN}(q_\pi^2) = \frac{\Lambda_\pi^2-m_\pi^2}{\Lambda_\pi^2-q_\pi^2}, \tag{13}$$

and

$$F_{Z\psi\pi}(q_\pi^2) = \frac{m_\psi^2-m_\pi^2}{m_\psi^2-q_\pi^2}, \tag{14}$$

where $\Lambda_\pi$ is the cutoff parameter for the $\pi NN$ vertex. In the next calculations, we take the typical value of $\Lambda_\pi = 0.7$ GeV as used in Refs. [52, 54, 58, 78].

As mentioned above, a higher photon beam energy is required for the production of charmoniumlike states through meson photoproduction process. Thus, to better describe the photoproduction of $Z_c^+(4200)$ at high photon energies we introduce a pion Reggeized treatment by replacing the Feynman propagator $\frac{1}{q_\pi^2 - m_\pi^2}$ with the Regge propagator as follows [57–59, 79],

$$\frac{1}{q_\pi^2 - m_\pi^2} \rightarrow \mathcal{R}_\pi = \left(\frac{s}{s_{\mathrm{scale}}}\right)^{\alpha_\pi(t)} \frac{\pi\alpha'_\pi}{\Gamma[1+\alpha_\pi(t)]} \frac{e^{-i\pi\alpha_\pi(t)}}{\sin[\pi\alpha_\pi(t)]}, \qquad (15)$$

where $\alpha'_\pi$ is the slope of the trajectory and the scale factor $s_{\mathrm{scale}}$ is fixed at 1 GeV$^2$, while $s = (p_1 + p_2)^2$ and $t = (p_2 + p_3)^2$ are the Mandelstam variables. In addition, the pionic Regge trajectory $\alpha_\pi(t)$ read as [58, 59, 79]

$$\alpha_\pi(t) = 0.7(t - m_\pi^2). \qquad (16)$$

The unpolarized differential cross section for the $Z_c^+(4200)$ photoproduction shown in Fig. 1(a) then reads

$$\frac{d\sigma}{d\cos\theta} = \frac{1}{32\pi s} \frac{\left|\vec{q}_z^{\,\mathrm{c.m.}}\right|}{\left|\vec{p}_1^{\,\mathrm{c.m.}}\right|} \left(\frac{1}{4}\sum_{spins} |\mathcal{A}|^2\right), \qquad (17)$$

where $\vec{p}_1^{\,\mathrm{c.m.}}$ and $\vec{q}_z^{\,\mathrm{c.m.}}$ are the three-momentum of initial photon and final $Z_c^+(4200)$ state, while $\theta$ denotes the angle of the outgoing $Z_c^+(4200)$ state relative to the photon beam direction in the c.m. frame. The total cross section can be easily obtained by integrating the above equation.

In Fig. 3, the total cross section $\sigma(\gamma p \rightarrow Z_c^+ n)$ through $\pi$ meson or pionic Regge trajectory exchange are presented with $\Lambda_\pi = 0.7$ GeV. Since the total cross section is proportional to the partial decay width $\Gamma_{Z(4200)\rightarrow J/\psi\pi}$, thus we note that the cross section changes by a factor of 3 to 4 when the partial width $\Gamma_{Z(4200)\rightarrow J/\psi\pi}$ is varied from 40.2 to 134.4 MeV. Besides, it is found that the total cross section through the Reggeized treatment is about five times smaller than that of result through a $\pi$ exchange, which indicate that the Reggeized treatment can lead to a lower cross section of the $Z_c^+(4200)$ photoproduction at high photon energies. Moreover, we note that the peak position of total cross section was moved to the higher energy point when the Reggeized treatment is used in the calculations.

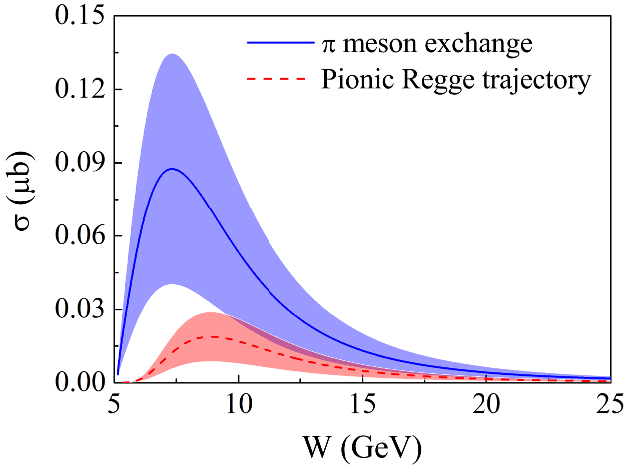

FIG. 3: (Color online) The total cross section for $\gamma p \rightarrow Z_c^+(4200)n$ process through $\pi$ meson or pionic Regge trajectory exchange. Here, the numerical results (the blue solid line and the red dashed line) correspond to the partial decay width $\Gamma_{Z_c(4200)\rightarrow J/\psi\pi} = 87.3$ MeV, while the bands stand for the uncertainties with the variation of $\Gamma_{Z_c(4200)\rightarrow J/\psi\pi}$ from 40.2 to 131.4 MeV.

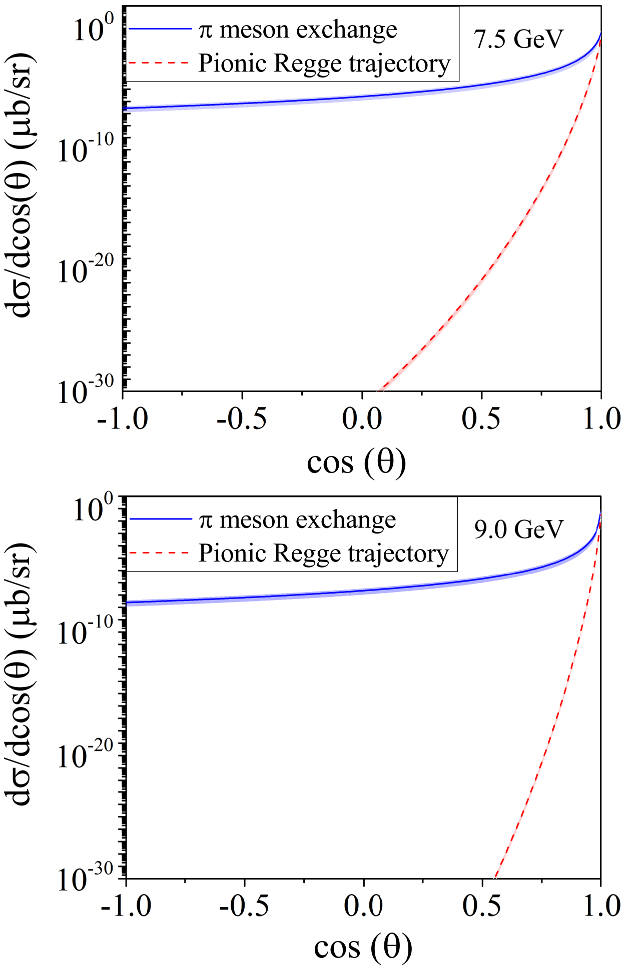

FIG. 4: (Color online) The differential cross section for $\gamma p \rightarrow Z_c^+(4200)n$ process through $\pi$ meson or pionic Regge trajectory exchange. The notation of the lines and bands as in Fig. 3.

Fig. 4 are the differential cross section for the $\gamma p \rightarrow Z_c^+ n$ process by exchanging the $\pi$ meson or pionic Regge trajectory at different energies, respectively. From Fig. 4 one can see that, relative to the results related to the $\pi$ exchange, the differential cross section by exchanging the pionic Regge trajectory are very sensitive to the $\theta$ angle and gives a considerable contribution at forward angles.

### C. Cross sections for the $\gamma p \to J/\psi \pi^+ n$ reaction

With the Feynman rules and above Lagrangian densities, we obtain the invariant scattering amplitude $\mathcal{M}_Z^{signal}$ for the $\gamma p \to J/\psi \pi^+ n$ process through $\pi$ exchange (as depicted in Fig. 1(b)) as follows,

$$\begin{aligned}\mathcal{M}_Z^{signal} &= (\sqrt{2} g_{\pi NN} \frac{g_{Z\psi\pi}}{M_Z} \frac{e}{f_\psi}) \bar{u}(p_3)\gamma_5 u(p_2) \\ &\times (p_1 \cdot q_\pi g^{\mu\alpha} - p_1^\alpha q_\pi^\mu)(p_4 \cdot p_5 g^{\rho\nu} - p_4^\rho p_5^\nu) \\ &\times \frac{1}{q_\pi^2 - m_\pi^2} G_Z^{\rho\alpha}(q_z) \epsilon_{\gamma\mu} \epsilon^*_{\psi\nu} \left( \frac{\Lambda_\pi^2 - m_\pi^2}{\Lambda_\pi^2 - q_\pi^2} \right) \\ &\times \left( \frac{m_\psi^2 - m_\pi^2}{m_\psi^2 - q_\pi^2} \right) \left( \frac{m_\psi^2 - M_Z^2}{m_\psi^2 - q_z^2} \right), \end{aligned} \tag{18}$$

where $G_Z^{\mu\alpha}$ are the propagators of the $Z(4200)$, taking the Breit-Wigner form [80],

$$G_Z^{\rho\alpha}(q) = \frac{-g_{\rho\alpha} + q_{z\rho} q_{z\alpha}/M_Z^2}{q_z^2 - M_Z^2 + i M_Z \Gamma_Z}. \tag{19}$$

Just as above practice, by replacing the Feynman propagator $\frac{1}{q_\pi^2 - m_\pi^2}$ with the Regge propagator $\mathcal{R}_\pi$, we can get the scattering amplitude for the $\gamma p \to J/\psi \pi^+ n$ process through the pionic Regge trajectory exchange.

Since the Pomeron can mediate the long-range interaction between a confined quark and a nucleon, thus $\gamma p \to J/\psi \pi^+ n$ via the Pomeron exchange (as described in Fig. 2) are the mainly background contribution to the $\gamma p \to Z_c^+(4200) n \to J/\psi \pi^+ n$ reaction. The invariant scattering amplitudes $\mathcal{M}_P^s$ and $\mathcal{M}_P^u$ for Figs. 2(a) and 2(b) can be written, respectively, as

$$\begin{aligned}\mathcal{M}_P^s &= 8\sqrt{2} \beta_c \mu_0^2 g_{\pi NN} F_N(q_s^2) \frac{F(t) G_P(s,t)}{(m_\psi^2 - t)(2\mu_0^2 + m_\psi^2 - t)} \\ &\times T^{\mu\rho\nu} \epsilon^*_{\psi\nu} \epsilon_{\gamma\mu} \bar{u}(p_3)\gamma_5 \frac{\not{q}_s + m_N}{q_s^2 - m_N^2} \gamma_\rho u(p_2), \end{aligned} \tag{20}$$

$$\begin{aligned}\mathcal{M}_P^u &= 8\sqrt{2} \beta_c \mu_0^2 g_{\pi NN} F_N(q_u^2) \frac{F(t) G_P(s,t)}{(m_\psi^2 - t)(2\mu_0^2 + m_\psi^2 - t)} \\ &\times T^{\mu\rho\nu} \epsilon^*_{\psi\nu} \epsilon_{\gamma\mu} \bar{u}(p_3)\gamma_\rho \frac{\not{q}_u + m_N}{q_u^2 - m_N^2} \gamma_5 u(p_2) \end{aligned} \tag{21}$$

with

$$G_P(s,t) = -i(\eta' s)^{\eta(t)-1} \tag{22}$$

where $\eta(t) = 1 + \epsilon + \eta' t$ is the Pomeron trajectory. Here, the concrete values $\epsilon = 0.08$ and $\eta' = 0.25$ GeV$^{-2}$ are adopted.

Considering the size of the hadrons, the monopole form factor for the off-shell intermediate nucleon is introduced as in the Bonn potential model [81]:

$$F_N(q_i^2) = \frac{\Lambda_N^2 - m_N^2}{\Lambda_N^2 - q_i^2}, \quad i = s, u \tag{23}$$

where $\Lambda_N$ and $q_i (q_s = p_3 + p_5, q_u = p_2 - p_5)$ are the cut-off parameter and four-momentum of the intermediate nucleon, respectively. For the value of $\Lambda_N$, we will discuss it in the next section. It is worth mentioning that the form factor is phenomenological and has a great uncertainty. Thus the dipole form factor is deserved to be discussed and compared with the monopole form.

Combining the signal terms and background amplitudes, we get the total invariant amplitude

$$\mathcal{M} = \mathcal{M}_Z^{signal} + \mathcal{M}_P^s + \mathcal{M}_P^u. \tag{24}$$

Thus the total cross section of the $\gamma p \to J/\psi \pi^+ n$ reaction could be obtained by integrating the invariant amplitudes in the three body phase space,

$$\begin{aligned} d\sigma(\gamma p \ \to \ J/\psi \pi^+ n) &= \frac{m_N^2}{|p_1 \cdot p_2|} \left( \frac{1}{4} \sum_{spins} |\mathcal{M}|^2 \right) \\ &\times (2\pi)^4 d\Phi_3(p_1 + p_2; p_3, p_4, p_5), \end{aligned} \tag{25}$$

where the three-body phase space is defined as [72]

$$d\Phi_3(p_1 + p_2; p_3, p_4, p_5) = \delta^4 \left( p_1 + p_2 - \sum_{i=3}^{5} p_i \right) \prod_{i=3}^{5} \frac{d^3 p_i}{(2\pi)^3 2E_i}. \tag{26}$$

## III. NUMERICAL RESULTS AND DISCUSSION

With the FOWL code in the CERN program library, the total cross section including both signal and background contributions can be calculated. In these calculations, the cutoff parameters $\Lambda_N$ related to the Pomeron term is a free parameter. Thus we first need to give a constraint on the value of $\Lambda_N$. Fig. 5 (a) and Fig. 5 (b) present the variation of cross section from the background contributions for $\gamma p \to J/\psi \pi^+ n$ with monopole and dipole form factor, respectively. It is obvious that the Pomeron exchange contributions with dipole form factor are more sensitive to the values of the cutoff $\Lambda_N$ than that of monopole form factor. Thus monopole form factor is adopted in the following calculation.

At present, no experiment data is available for the $\gamma p \to J/\psi \pi^+ n$ process. However, we notice that the similar reaction $\gamma p \to J/\psi p$ and $\bar{p} p \to J/\psi \pi^0$ have been measured by some experiment [82–85], where the measured cross sections of these two process are about 1 nb and 10 nb, respectively. Here, we naively think that the cross section of $\gamma p \to J/\psi \pi^+ n$ may be equal to or less than that of $\gamma p \to J/\psi p$, while it greater than that of $\bar{p} p \to J/\psi \pi^0$. Thus we constrain the cutoff to be $\Lambda_N = 0.96$ GeV as used in Ref. [54, 55], which will be used in our calculations.

To better understand that the effects of Reggeized treatment on the final results, we calculate the total cross section of the $\gamma p \to J/\psi \pi^+ n$ reaction without or with Reggeized treatment as presented in Fig. 6 and Fig. 7, respectively.

Fig. 6 show the total cross sections for $\gamma p \to J/\psi \pi^+ n$ reaction including both $\pi$ exchange and Pomeron exchange contributions by taking $\Lambda_Z = 0.7$ GeV and $\Lambda_N = 0.96$ GeV. We

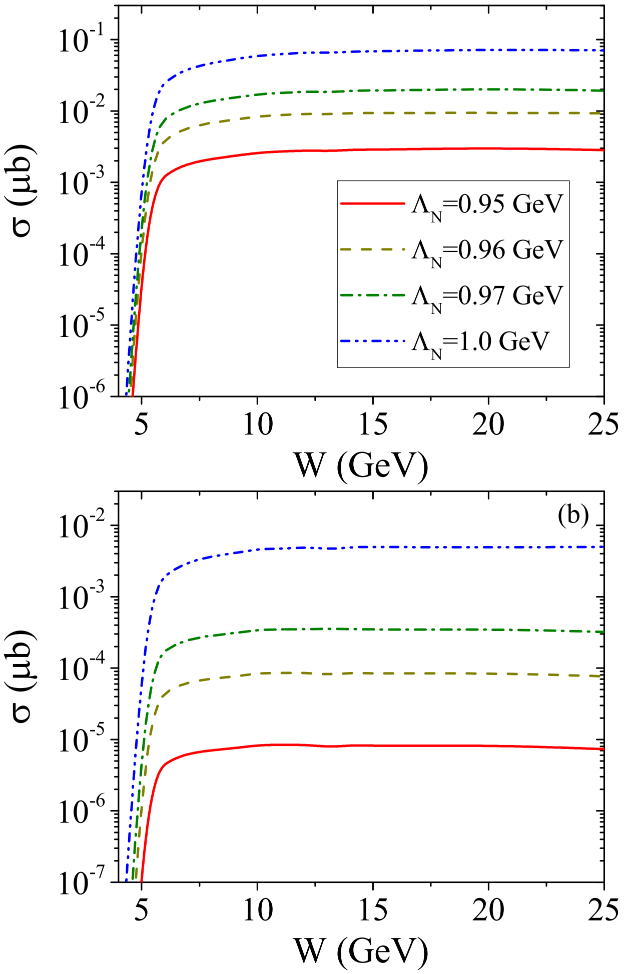

FIG. 5: (Color online) (a): The cross section of background from the Pomeron exchange for $\gamma p \to J/\psi\pi^+ n$ process with monopole form factor at the different values of the cutoff parameter $\Lambda_N$. (b) is same as the (a), but for the case of dipole form factor.

notice that the line shape of total cross section goes up very rapidly and has a peak around $W \simeq 7.5$ GeV. In this energy region, the cross section of signal are larger than that of background when taking the partial width values $\Gamma_{Z_c(4200)\to J/\psi\pi} = 87.3$ or 134.4 MeV.

In contrast, Fig. 7 present the total cross sections for $\gamma p \to J/\psi\pi^+ n$ reaction including both pionic Regge trajectory exchange and Pomeron exchange contributions by taking $\Lambda_Z = 0.7$ GeV and $\Lambda_N = 0.96$ GeV. It is found that the total cross section shows a peak at center of mass energy $W \simeq 9$ GeV, and the contributions from signal are driven down when using the Reggeized treatment. We note that the cross section of signal just a little bit higher than that of background at center of mass energy $W \simeq 9$ GeV even a larger partial decay width value ($\Gamma_{Z_c(4200)\to J/\psi\pi} = 134.4$ MeV) are adopted.

To demonstrate the feasibility of searching for the charged charmoniumlike $Z_c^+(4200)$ through the $\gamma p \to J/\psi\pi^+ n$ reaction, we further give the Dalitz plot and invariant mass spectrum for the $\gamma p \to J/\psi\pi^+ n$ process.

Fig. 8 present the Dalitz plot and $J/\psi\pi^+$ invariant mass spectrum for the $\gamma p \to J/\psi\pi^+ n$ process with the Reggeized treatment at different center of mass energy, where the numerical results are obtained by taking the partial decay width $\Gamma_{Z_c(4200)\to J/\psi\pi} = 134.4$ MeV. From Dalitz plot we notice that there exist a vertical band and a horizontal band, which are from the signal and background contributions, respectively. Moreover, one notice that the signal of $Z_c^+(4200)$ with $W = 9.0$ is more explicit than that with $W = 7.5$ or 12 GeV, which is consistent with the result in Fig. 7. Thus we can conclude that the $W = 9.0$ GeV is the best energy window for searching for the charged $Z_c^+(4200)$ via the $\gamma p \to J/\psi\pi^+ n$ process. By analyzing the $J/\psi\pi^+$ invariant mass spectrum in Fig. 8, one finds that the number of events of $J/\psi\pi^+$ can reach up to 500/2 GeV$^2$ at $W = 9.0$ GeV when taking 50 million collisions of $\gamma p$.

Moreover, we take the center of mass energy $W = 9.0$ GeV as one of the inputs to calculate the Dalitz plot and $J/\psi\pi^+$ invariant mass spectrum related to the smaller partial decay width, which are presented in Fig. 9. From Dalitz plot in Fig. 9 we notice that there exist an clear vertical band which related to the $Z_c^+(4200)$ signal when taking partial decay width $\Gamma_{Z_c(4200)\to J/\psi\pi} = 87.3$ MeV. Since the signal and background contribution do not interfere with each other as shown in Dalitz plot, the signal of $Z_c^+(4200)$ can also be distinguished from the background. Thus we can expect about 375/2 GeV$^2$ events for the production of $J/\psi\pi^+$ in 50 million collisions of $\gamma p$ at $W = 9.0$ GeV if taking $\Gamma_{Z_c(4200)\to J/\psi\pi} = 87.3$ MeV, which is enough to meet the requirements of the experiment. However, we also see that the signal of $Z_c^+(4200)$ are submerged in the background and will be difficult to distinguish it from the background if taking $\Gamma_{Z_c(4200)\to J/\psi\pi} = 40.2$ MeV.

For comparison, we calculate the Dalitz plot and $J/\psi\pi^+$ invariant mass spectrum for the $\gamma p \to J/\psi\pi^+ n$ process with-

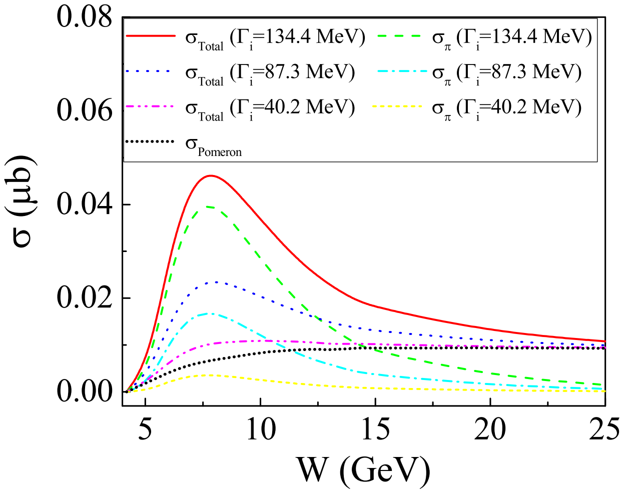

FIG. 6: (Color online) The energy dependence of the total cross sections for the $\gamma p \to J/\psi\pi^+ n$ reaction. Here, $\sigma_{Pomeron}$ and $\sigma_\pi$ denote the results via the Pomeron and $\pi$ exchange, respectively, while $\sigma_{Total}$ is the total cross section of $\gamma p \to J/\psi\pi^+ n$. The variation of $\sigma_\pi$ and $\sigma_{Total}$ to $W$ with several typical partial width values $\Gamma_{Z(4200)\to J/\psi\pi} = 40.2, 87.3, 134.4$ MeV are also presented.

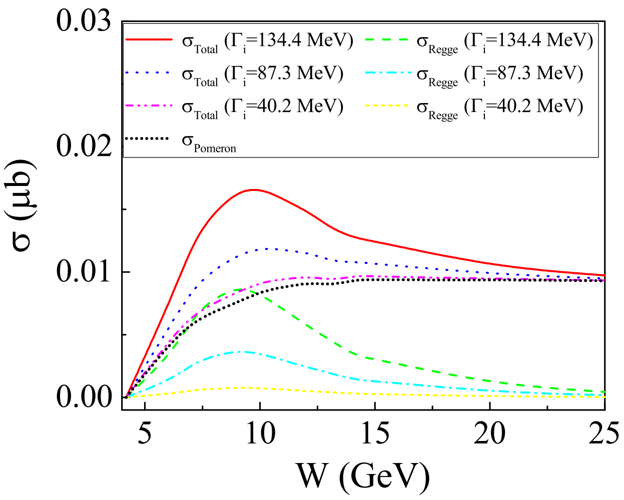

FIG. 7: (Color online) The energy dependence of the total cross sections for the $\gamma p \to J/\psi\pi^+ n$ reaction. Here, $\sigma_{Pomeron}$ and $\sigma_{Regge}$ denote the results via the Pomeron exchange and pionic Regge trajectory exchange, respectively, while $\sigma_{Total}$ is the total cross section of $\gamma p \to J/\psi\pi^+ n$. The variation of $\sigma_{Regge}$ and $\sigma_{Total}$ to $W$ with several typical partial width values $\Gamma_{Z(4200)\to J/\psi\pi} = 40.2, 87.3, 134.4$ MeV are also presented.

out the Reggeized treatment at $W = 7.5$ GeV, as presented in Fig. 10. One finds that a vertical band related to the signal of $Z_c^+(4200)$ appears in Dalitz plot even if the lowest partial decay width ($\Gamma_{Z_c(4200)\to J/\psi\pi} = 40.2$ MeV) is adopted, which is obvious different from that with Reggeized treatment.

## IV. UPPER LIMIT OF THE DECAY WIDTH $\Gamma_{Z_c(4200)\to J/\psi\pi}$

The $J/\psi\pi^\pm$ mass spectrum presented by the COMPASS collaboration in [56], which studied exclusive photoproduction of a $J/\psi\pi^\pm$ state at a nuclear target in the range from 7 GeV to 19 GeV in the centre-of-mass energy of the photon-nucleon system, does not exhibit any statistically significant structure at about 4.2 GeV. Nevertheless it can be used for estimation of an upper limit for the value $BR(Z_c(4200) \to J/\psi\pi) \times \sigma_{\gamma N\to Z_c(4200)N}$.

A sum of two exponential functions for a continuum and a Breit-Wigner curve for a possible contribution of $Z_c^\pm(4200)$ photoproduction was fitted to the mass spectrum in the range from 3.4 GeV to 6.0 GeV. The mass $M_{Z_c(4200)} = 4196$ MeV and the width $\Gamma_{Z_c(4200)} = 370$ MeV were used as the fixed parameters. Doing this we ignore possible contribution of any other resonances like $Z_c(3900)$ and their interference with $Z_c(4200)$. The $J/\psi\pi^\pm$ mass spectrum with the fitting curve is shown in Fig. 11. The obtained from the fit possible number of $Z_c(4200)$ events is $N_{Z_c(4200)} = 58\pm31$. It can be converted to the upper limit $N^{UL}_{Z_c(4200)} < 98$ events corresponding to a confidence level of CL = 90%. According to the normalization used in [56] this limit corresponds to the result

$$BR(Z_c(4200) \to J/\psi\pi) \times \sigma_{\gamma N\to Z_c(4200)N} < 340 \text{ pb}. \tag{27}$$

This result can be used for estimation of an upper limit for the partial width $\Gamma_{J/\psi\pi}$ of the decay $Z_c(4200) \to J/\psi\pi$ based on the Reggeized treatment. The production cross section, averaged over the $W$-range covered by COMPASS, is about $\Gamma_{J/\psi\pi} \times 91$ pb/MeV. So

$$\frac{\Gamma_{J/\psi\pi}}{\Gamma_{tot}} \times \sigma_{\gamma N\to Z_c^\pm(4200)\ N} = \frac{\Gamma^2_{J/\psi\pi} \times 90 \text{ pb/MeV}}{\Gamma_{tot}} < 340 \text{ pb}. \tag{28}$$

Assuming $\Gamma_{\text{tot}} = 370$ MeV, we obtain an upper limit $\Gamma_{J/\psi\pi} < 37$ MeV.

Photoproduction of the $Z_c^+(4200)$ state could also be tested using the data on the HERMES experiment. It covers the range 2 GeV$< W < 6.3$ GeV [86] where the difference between production cross sections calculated through pionic Regge trajectory exchange and virtual pion exchange is maximal.

## V. SUMMARY

In this work, we study the charged $Z_c(4200)$ production in $\gamma p \to J/\psi\pi^+ n$ reaction with an effective Lagrangian approach and the Regge trajectories model. Since the charmoniumlike $Z_c(4200)$ was only observed in $B$ meson decay process, it is an interesting and important topic to study the charmoniumlike $Z_c(4200)$ by different processes.

Through of analysis and comparison, our numerical results indicate:

(I) The effect of introducing the Reggeized treatment has been to significantly reduce the magnitude of cross section for the $Z_c(4200)$ photoproduction. The total cross section for the $\gamma p \to Z_c^+(4200)n$ via pionic Regge trajectory exchange is smaller than that of without Reggeized treatment and the predictions in Refs. [52–55].

(II) We finds that the differential cross section for the $\gamma p \to Z_c^+(4200)n$ by exchanging the pionic Regge trajectory are very sensitive to the $\theta$ angle and gives a considerable contribution at forward angles, which can be checked by further experiment and may be an effective way to examine the validity of the Reggeized treatment.

(III) The total cross section for the $\gamma p \to J/\psi\pi^+ n$ process with Reggeized treatment is lower than that of without Reggeized treatment. The calculations indicate that the partial decay width $\Gamma_{Z_c(4200)\to J/\psi\pi}$ is a key parameter in studying the production of $Z_c(4200)$ via $\gamma p$ collision. Adopting the partial decay width predicted in Ref. [43] by assuming that the $Z_c(4200)$ is a tetraquark state, we find that the signal of $Z_c^+(4200)$ can also be distinguished from the background at $W = 9.0$ GeV if taking $\Gamma_{Z_c(4200)\to J/\psi\pi} = 87.3$ MeV, but not for the case of taking $\Gamma_{Z_c(4200)\to J/\psi\pi} = 40.2$ MeV. In Ref. [48], by assuming the $Z_c(4200)$ as an axial-vector molecule-like state, the partial decay width $\Gamma_{Z_c(4200)\to J/\psi\pi} = 24.6$ MeV was obtained with QCD sum rule. If the predicted

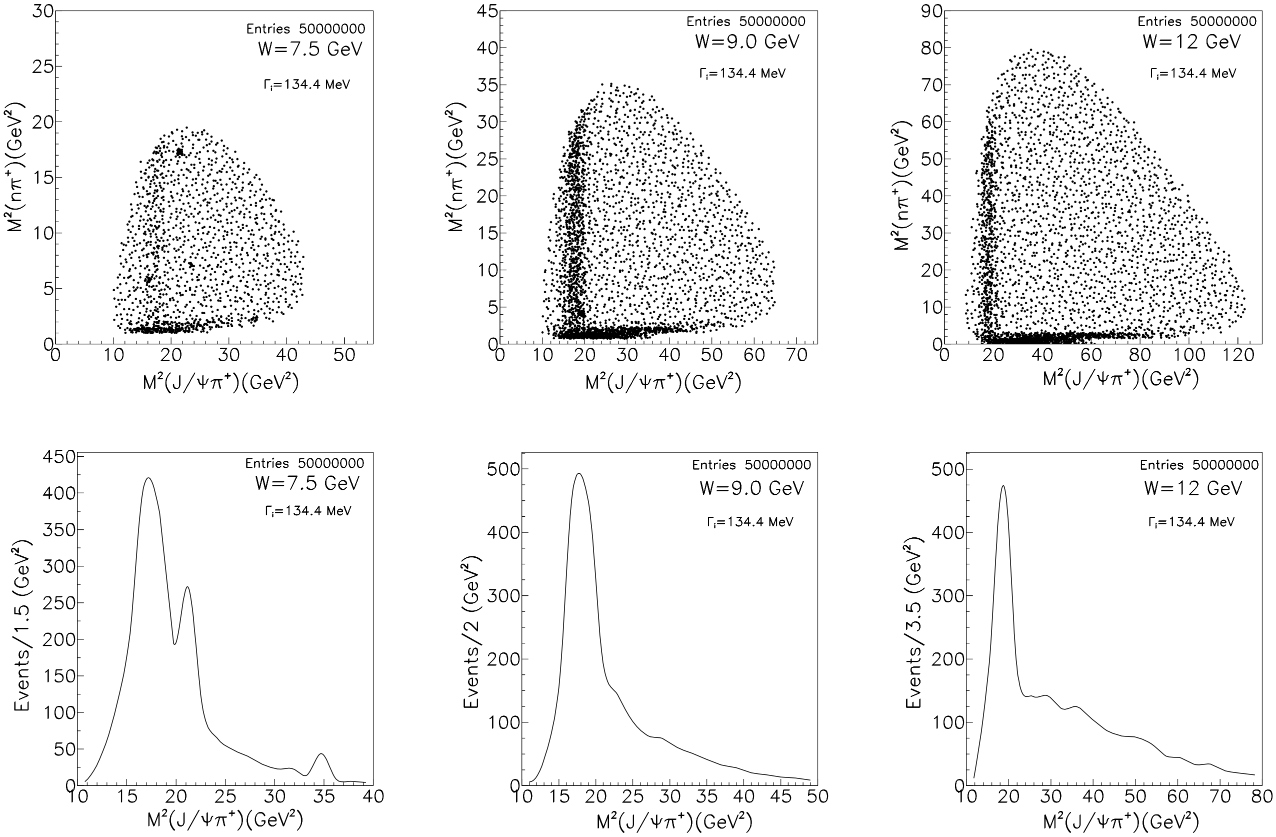

FIG. 8: (Color online) The Dalitz plot (top) and the $J/\psi\pi^+$ invariant mass spectrum (bottom) for the $\gamma p \to J/\psi\pi^+ n$ reaction with the Reggeized treatment at different center of mass energy $W = 7.5, 9, 12$ GeV. Here, the numerical result corresponds to the partial decay width $\Gamma_{Z(4200)\to J/\psi\pi} =$ 134.4 MeV.

$\Gamma_{Z_c(4200)\to J/\psi\pi} = 24.6$ MeV in Ref. [48] is reliable, then the signal of $Z_c^+(4200)$ produced in $\gamma p$ collision will be difficult to be distinguished from background. Thus the experiment of the meson photoproduction of $Z_c(4200)$ may provide a useful adjunctive information for the confirmation of the inner structure of $Z_c(4200)$.

(IV) The peak position of total cross section for the $\gamma p \to Z_c^+(4200)n \to J/\psi\pi^+ n$ process was moved to the higher energy point when adding the Reggeized treatment, which means that a higher beam energy is necessary for the meson photoproduction of $Z_c(4200)$. The results show that $W \simeq 9.0$ GeV is the best energy window for searching for the $Z_c(4200)$ via $\gamma p$ collision. All these calculations can be checked in the future experiment.

(V) Using data on exclusive photoproduction of a $J/\psi\pi^\pm$ state from COMPASS we estimated the upper limit for the value of $Z_c(4200)$ production cross section multiplied by the branching ratio of the $Z_c(4200) \to J/\psi\pi$ decay to be above 340 pb (CL=90 %). According to the Reggeized treatment it corresponds to the upper limit of $\Gamma_{Z_c(4200)\to J/\psi\pi}$ of about 37 MeV, which is coincidence with the prediction of $\Gamma_{Z_c(4200)\to J/\psi\pi} = 24.6$ MeV by assuming the $Z_c(4200)$ as a molecule-like state in [48].

Since the Reggeized treatment used in this work has been proven to be more precise than the general effective Lagrangian approach in the pion and kaon photoproduction [57–59], our theoretical results may provide a valuable information, both for searching for the $Z_c(4200)$ via $\gamma p$ collision or explaining the lack of observation of $Z_c(4200)$ in experiment. Therefore, the more experiment about the photoproduction of $Z_c(4200)$ are suggested, which will be important to improve our knowledge of the nature of $Z_c(4200)$ and the Regge theory.

## VI. ACKNOWLEDGMENTS

The authors would like to acknowledge the COMPASS collaboration for allowing us to use the data of $J/\psi\pi^\pm$ mass spectrum. Meanwhile, X. Y. W. is grateful Dr. Qing-Yong Lin for the valuable discussions and help. This work is partly supported by the National Basic Research Program (973 Program Grant No. 2014CB845406), the National Natural Science Foundation of China (Grant No. 11175220) and the One Hundred Person Project of the Chinese Academy of Science (Grant No. Y101020BR0).

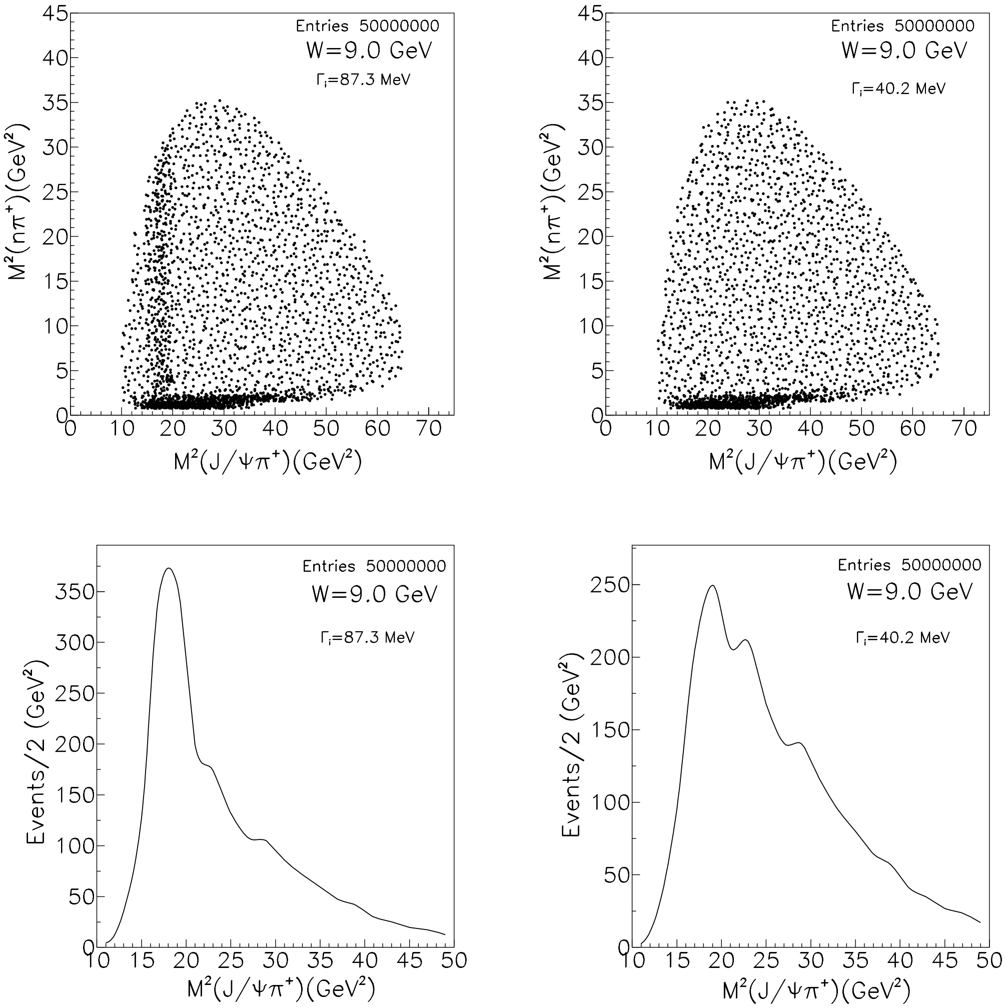

FIG. 9: (Color online) The Dalitz plot (top) and the $J/\psi\pi^+$ invariant mass spectrum (bottom) for the $\gamma p \to J/\psi\pi^+ n$ reaction with the Reggeized treatment at center of mass energy $W = 9$ GeV. Here, the numerical results correspond to the partial decay width values $\Gamma_{Z(4200)\to J/\psi\pi} = 87.3, 40.2$ MeV.

---

[1] S. K. Choi *et al.* (Belle Collaboration), Phys. Rev. Lett. 91, 262001 (2003).

[2] R. Aaij *et al.* (LHCb Collaboration), Phys. Rev. Lett. 110, 222001 (2013).

[3] B. Aubert *et al.* (BARBAR Collaboration), Phys. Rev. Lett. 95, 142001 (2005).

[4] C. Z. Yuan *et al.* (Belle Collaboration), Phys. Rev. Lett. 99, 182004 (2007).

[5] M. Ablikim *et al.* (BESIII Collaboration), Phys. Rev. Lett. 110, 252001 (2013).

[6] Z. Q. Liu *et al.* (Belle Collaboration), Phys. Rev. Lett. 110, 252002 (2013).

[7] M. Ablikim *et al.* (BESIII Collaboration), Phys. Rev. Lett. 112, 132001 (2014).

[8] M. Ablikim *et al.* (BESIII Collaboration), Phys. Rev. Lett. 111, 242001 (2013).

[9] R. Mizuk *et al.* (Belle Collaboration), Phys. Rev. D 78, 072004 (2008).

[10] S. K. Choi *et al.* (Belle Collaboration), Phys. Rev. Lett. 100, 142001 (2008).

[11] K. Chilikin *et al.* (Belle Collaboration), Phys. Rev. D 88, 074026 (2013).

[12] R. Aaij *et al.* (LHCb Collaboration), Phys. Rev. Lett. 112, 222002 (2014).

[13] K. Chilikin *et al.* (Belle Collaboration), Phys. Rev. D 90, 112009 (2014).

[14] A. Bondar *et al.* (Belle Collaboration), Phys. Rev. Lett. 108, 122001 (2012).

[15] I. Adachi *et al.* (Belle Collaboration), Phys. Rev. Lett. 108, 032001 (2012).

[16] I. Adachi *et al.* (Belle Collaboration), arXiv:1105.4583.

[17] X. Liu, Chin. Sci. Bull. 59, 3815 (2014).

[18] A. Esposito, A. L. Guerrieri, F. Piccinini, A. Pilloni and A. D. Polosa, Int. J. Mod. Phys. A 30, 1530002 (2014).

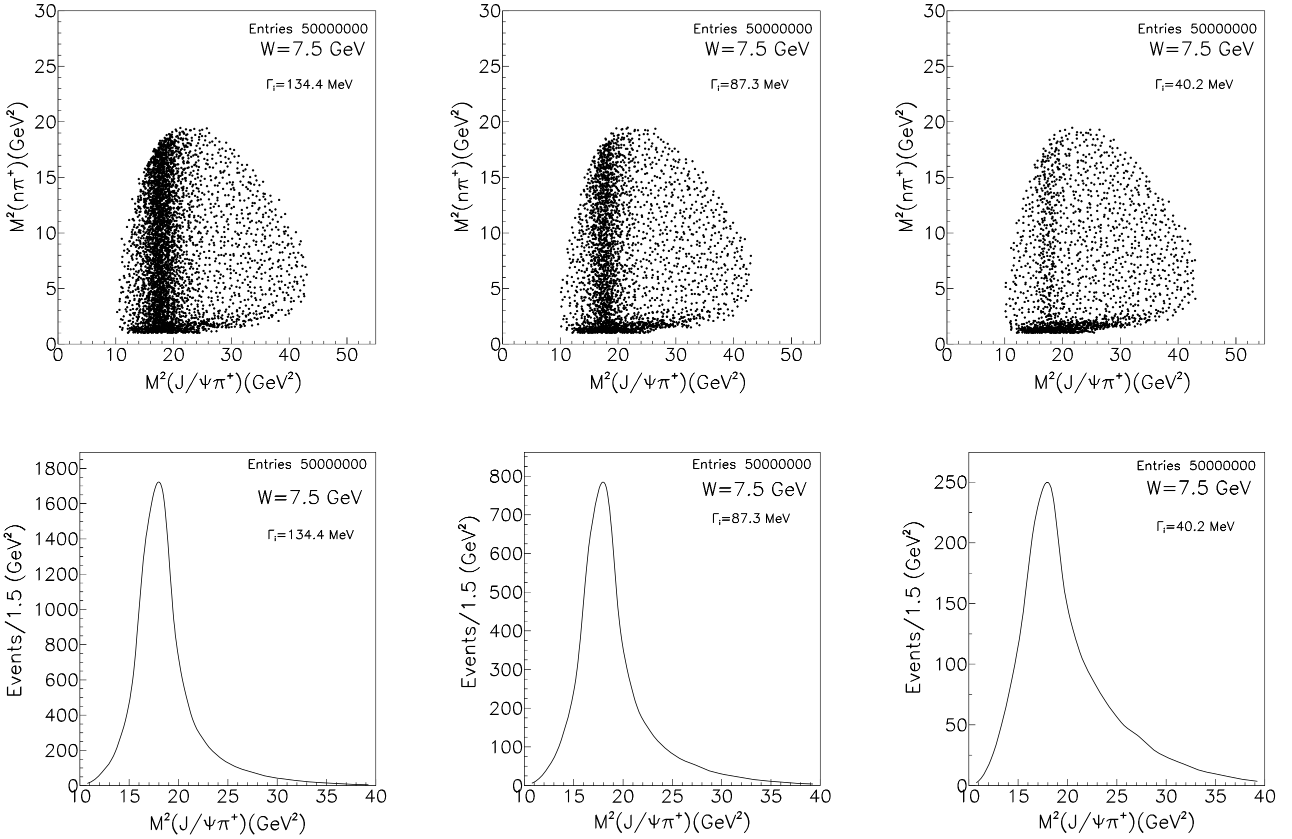

FIG. 10: (Color online) The Dalitz plot (top) and the $J/\psi\pi^+$ invariant mass spectrum (bottom) for the $\gamma p \to J/\psi\pi^+ n$ reaction without the Reggeized treatment at center of mass energy $W = 7.5$ GeV. Here, the numerical results correspond to the partial decay width values $\Gamma_{Z(4200)\to J/\psi\pi} = 134.4, 87.3, 40.2$ MeV.

[19] S. L. Olsen, Hyperfine Interact. 229, 7 (2014).

[20] M. Nielsen, F. S. Navarra and S. H. Lee, Phys. Rept. 497, 41 (2010).

[21] M. Nielsen and F. S. Navarra, Mod. Phys. Lett. A 29, 1430005 (2014).

[22] T. Xiao *et al.*, Phys. Lett. B 727, 366 (2013).

[23] P. Krokovny *et al.* (Belle Collaboration), Phys. Rev. D 88, 052016 (2013).

[24] M. Ablikim *et al.* (BESIII Collaboration), Phys. Rev. Lett. 113, 212002 (2014).

[25] S. L. Zhu, Phys. Lett. B 625, 212 (2005).

[26] Y.-R. Liu *et al.*, Phys. Rev. D 82, 014011 (2010).

[27] N. Li and S.-L. Zhu, Phys. Rev. D 86, 074022 (2012).

[28] H. Hogaasen, J. M. Richard, and P. Sorba, Phys. Rev. D 73, 054013 (2006).

[29] D. Ebert, R. N. Faustov, and V. O. Galkin, Phys. Lett. B 634, 214 (2006).

[30] N. Barnea, J. Vijande, and A. Valcarce, Phys. Rev. D 73, 054004 (2006).

[31] Q. Wang, C. Hanhart, and Q. Zhao, Phys. Rev. Lett. 111, 132003 (2013).

[32] E. Braaten, Phys. Rev. Lett. 111, 162003 (2013).

[33] D. Y. Chen, X. Liu, and T. Matsuki, Phys. Rev. D 88, 036008 (2013).

[34] C. F. Qiao and L. Tang, Eur. Phys. J. C 74, 2810 (2014).

[35] F. Aceti, M. Bayar, and E. Oset, Eur. Phys. J. A 50, 103 (2014).

[36] I. V. Danilkin, V. D. Orlovsky and Yu. A. Simonov, Phys. Rev. D 85, 034012 (2012).

[37] D. Bugg, Europhys. Lett. 96, 11002 (2011).

[38] R. D. Matheus, *et al.*, Phys. Rev. D 75, 014005 (2007).

[39] L. Maiani *et al.*, Phys. Rev. D 89, 114010 (2014).

[40] L. Zhao, W. Z. Deng and S. L. Zhu, Phys. Rev. D 90, 094031 (2014).

[41] W. Chen and S. L. Zhu, Phys. Rev. D 83, 034010 (2011).

[42] W. Chen and S. L. Zhu, EPJ Web Conf. 20, 01003 (2012).

[43] W. Chen *et al.*, arXiv:1501.03863 [hep-ph].

[44] J. J. Wu, R. Molina, E. Oset and B. S. Zou, Phys. Rev. Lett. 105, 232001 (2010).

[45] J. J. Wu, R. Molina, E. Oset and B. S. Zou, Phys. Rev. C 84, 015202 (2011).

[46] X. Y. Wang and X. R. Chen, Europhys. Lett. 109, 41001 (2015).

[47] X. Y. Wang and X. R. Chen, Eur. Phys. J. A 51, 85 (2015).

[48] Z. G. Wang, arXiv:1502.01459.

[49] H. W. Ke and X. Liu, Eur. Phys. J. C 58, 217 (2008).

[50] X. Y. Wang, J. J. Xie and X. R. Chen, Phys. Rev. D 91, 014032 (2015).

[51] X. Y. Wang, X. R. Chen, Adv. High Energy Phys. 2015, 918231 (2015).

[52] X. H. Liu, Q. Zhao, and F. E. Close, Phys. Rev. D 77, 0944005 (2008).

[53] J. He and X. Liu, Phys. Rev. D 80, 114007 (2009).

[54] Q. Y. Lin *et al.*, Phys. Rev. D 88, 114009 (2013).

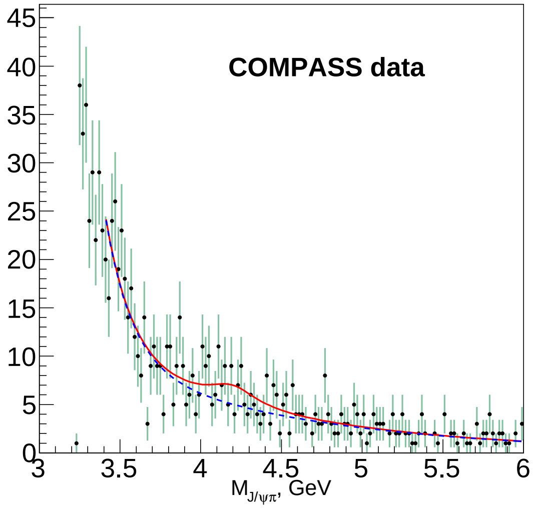

FIG. 11: (Color online) Mass spectrum of the $J/\psi\pi$ state obtained by COMPASS [56]. The fitted function is shown as a red solid line. Dashed blue line corresponds to the continuum description.

[55] Q. Y. Lin *et al.*, Phys. Rev. D 89, 034016 (2014).
[56] C. Adolph *et al.* (COMPASS Collaboration), Phys. Lett. B 742, 330 (2015).
[57] M. Guidal, J. M. Laget, and M. Vanderhaeghen, Nucl. Phys. A 627, 645 (1997).
[58] G. Galatà, Phys. Rev. C 83, 065203 (2011).
[59] J. He, Phys. Rev. C 89, 055204 (2014).
[60] A. B. Kaidalov *et al.*, Eur. Phys. J. C 47, 385 (2006).
[61] V. A. Khoze, A. D. Martin and M. G. Ryskin, Eur. Phys. J. C 48, 797 (2006).
[62] S. Chekanov, *et al.* (ZEUS Collaboration), Nucl. Phys. B 637, 3 (2002).
[63] B. Z. Kopeliovich, B. Povh and I. Potashnikova, Z. Phys. C 73, 125 (1996).
[64] H. Holtmann, *et al.*, Phys. Lett. B 338, 393 (1995).
[65] M. Burkardt *et al.*, Phys. Rev. D 87, 056009 (2013).
[66] Y. Salamu *et al.*, Phys. Rev. Lett. 114, 122001 (2015).
[67] F. Carvalho *et al.*, arXiv:1507.07758.
[68] K. Tsushima, S. W. Huang, and A. Faessler, Phys. Lett. B 337, 245 (1994).
[69] K. Tsushima, *et al.*, Phys. Lett. B 411, 9 (1997), Erratum-ibid. Phys. Lett. B 421, 413 (1998).
[70] K. Tsushima, *et al.*, Phys. Rev. C 59, 369 (1999), Erratum-ibid. Phys. Rev. C 61, 029903 (2000).
[71] Z. Lin, C. M. Ko, and B. Zhang, Phys. Rev. C 61, 024904 (2000).
[72] K. A. Olive *et al.* (Particle Data Group), Chin. Phys. C, 38, 090001 (2014).
[73] T. Bauer and D. R. Yennie, Phys. Lett. 60B, 165 (1976).
[74] T. Bauer and D. R. Yennie, Phys. Lett. 60B, 169 (1976).
[75] T. H. Bauer, *et al.*, Rev. Mod. Phys. 50, 261 (1978); 51, 407(E) (1979).
[76] A. Donnachie and P. V. Landshoff, Phys. Lett. B 185, 403 (1987).
[77] M. A. Pichowsky and T. S. H. Lee, Phys. Lett. B 379, 1 (1996).
[78] V. P. Goncalves and M. L. L. da Silva, Phys. Rev. D 89, 114005 (2014).
[79] R. J. Eden, Rep. Prog. Phys. 34, 995 (1971).
[80] W. H. Liang, P. N. Shen, J. X. Wang and B. S. Zou, J. Phys. G 28, 333 (2002).
[81] R. Machleidt, K. Holinde, and Ch. Elster, Phys. Rep. 149, 1 (1987).
[82] https://www.jlab.org/Hall-C/talks/08_21_06/Chudakov.pdf.
[83] A. Levy, arXiv:0711.0737.
[84] T. A. Armstrong *et al.*, Phys. Rev. Lett. 69, 2337 (1992).
[85] M. Andreotti *et al.*, Phys. Rev. D 72, 032001 (2005); D. Joffe, arXiv:hep-ex/0505007.
[86] A. Movsisyan, EPJ Web Conf. 73 (2014) 02017 (2014)